Viewpoints

Biochemical pH clamp: the forgotten resource in membrane bioenergetics

Summary

Solute uptake and release by plant cells are frequently energized by coupling to H^+ influx supported by the proton motive force (pmf). The pmf results from a stable pH difference between the apoplast and the cytosol, with bulk values ranging from 4.9 to 5.8 and from 7.1 to 7.5, respectively, in combination with a negative electrical membrane potential. The P-type H^+ ATPases pumping H^+ from the cytosol into the apoplast at the expense of ATP hydrolysis are generally viewed as the only pmf source, exclusively linking membrane transport to energy metabolism. However, recent evidence suggests that pump activity may be insufficient to energize transport, particularly under stress conditions. Indeed, cytosolic H^+ scavenging and apoplastic H^+ generation by metabolism (denoted as 'active' buffering in contrast to the readily exhausted 'passive' matrix buffering) also stabilize the pH gradient. In the cytosol, H^+ scavenging is mainly associated with malate decarboxylation catalyzed by malic enzyme, and via the GABA shunt of the tricarboxylic acid (TCA) cycle involving glutamate decarboxylation. In the apoplast, formation of bicarbonate from CO_2, the end-product of respiration, generates H^+ at pH ≥ 6. Membrane potential is stabilized by K^+ release and/or by anion uptake via ion channels. Finally, thermodynamic aspects of active buffering are discussed.

Introduction

Interest in membrane bioenergetics has recently re-awakened in the plant sciences, and the consensus on this issue, that prevailed for several decades and is reflected in the textbooks (Taiz & Zeiger, 2010), has come under debate again. The interplay of various transporters co-localized in the plasma membrane and in the tonoplast apparently gives rise to futile cycling of solutes, particularly under salt stress (Munns *et al.*, 2019; Shabala *et al.*, 2019). Maintenance of ionic gradients under these conditions is associated with an enormous 'waste' of energy that seems to exceed the capacities of cell metabolism. Measurements of unidirectional Na^+ fluxes under salinity stress with radioactive tracers provided evidence for rapid transmembrane sodium cycling (RTSC) across the plasma membrane of root epidermal and cortical cells. RTSC was calculated to impose a huge energy drain on the plant (Malagoli *et al.*, 2008) which prompted Britto & Kronzucker (2015) to question the experimental evidence altogether; ^{22}Na flux data were interpreted as a result of ion exchange processes in the cell walls instead. Recently, discussion was also stimulated on the molecular mechanisms of water transport across membranes, which is generally assumed to be passive, following the transmembrane water potential gradient. Recently, though, an alternative mechanism for water transport by coupling to solute transport was proposed (Raven & Doblin, 2014; Wegner, 2014, 2015, 2017); the model includes circular solute fluxes to maintain their (electro)chemical potential gradient, at the expense of metabolic energy. For the generation of a root pressure such mechanism of secondary active water transport appears to be feasible from an energetic point of view (Fricke, 2015; Wegner, 2015), even though it is a considerable energetic burden for the plant. Interestingly, RTSC was also suggested to be involved in water uptake under saline conditions via dual-function aquaporins that transport both Na^+ and water (Byrt *et al.*, 2017), thus partly alleviating the associated osmotic stress (Munns *et al.*, 2019).

The bioenergetics of plant membrane transport is currently based on a central dogma: maintenance of (electro)chemical gradients across the membrane is tightly linked to the activity of proton pumps that operate as the exclusive interface to metabolism. As such, H^+ pumps were classified as master enzymes of membrane transport (Serrano, 1989). For the plasma membrane and the tonoplast this role is ascribed to the P-type and the V-type ATPases, respectively, the latter being assisted by the PPase (other ATPases are of little relevance for membrane bioenergetics). This dogma is challenged here on the grounds that, strictly speaking, it is not the pump activity *per se* which is used to energize other transport processes. Rather, it is the proton motive force (pmf) which is defined as the electrochemical potential difference for H^+ divided by the Faraday constant. The pmf consists of a pH difference across the membrane and an electrical potential gradient. So far it was tacitly assumed that H^+ pump activity is indispensable for establishing and maintaining a pmf, despite long-standing evidence for the existence of pH gradients across the plasma membrane even in the absence of proton pump activity (exemplified in detail later). This is due to the 'biochemical pH stat' preventing acidification of the cytosol when H^+ influx exceeds H^+ extrusion by the P-ATPase (also addressed as the 'biophysical pH stat'; Raven & Smith, 1976). In addition to the transient 'passive' buffer capacity of the cytosol, sustainable 'active' buffering occurs due to permanent H^+ consumption by metabolism (which is eventually driven by photosynthesis in green tissues). Apoplastic pH is also buffered, although apparently less effectively than the cytosol. Moreover, it was shown experimentally that the membrane potential remains in the negative voltage range under these conditions (even though the cell is strongly depolarized with respect to transport dominated by H^+ pump activity), indicating that a significant pmf is retained.

New Phytologist

Therefore, for a ΔpH of 1 and a membrane potential of −20 mV, a pmf of −79 mV (at room temperature) is calculated that is available to perform work, e.g. to transport other solutes in the 'uphill' direction. Even though a large body of experimental evidence has been accumulated on biochemical pH stat mechanisms in the last decades (see later), discussion was restricted to pH regulation, and cytosolic pH as a second messenger (Felle, 2001). Surprisingly, to the best of our knowledge, the role of active pH buffering for membrane bioenergetics has not been considered yet. This gap is filled here. Initially, the experimental evidence for membrane transport being energized by active apoplastic and cytosolic pH buffering, giving rise to a 'biochemical pH clamp' across the plasma membrane, is summarized. Subsequently, the biochemical pathways involved in pH buffering are discussed. Finally, some thermodynamic considerations are presented. The investigation focuses on sink tissue, primarily on roots, where energy shortage is potentially more pertinent than in leaves. However, it is limited to tissues sufficiently provided with oxygen to perform oxidative phosphorylation. Cases of anoxia and severe hypoxia have been covered recently in a comprehensive review by Greenway & Armstrong (2018) and will not be discussed here.

Evidence for H^+ influx across the plasma membrane sustained by an active buffering of cytosolic and apoplastic pH

Cytosolic and apoplastic pH (pH_c and pH_a, respectively) have been extensively studied in the last four decades using various techniques, among them H^+ selective microelectrodes, P_i NMR spectroscopy, distribution of weak acids, fluorescent dyes like FITC and BCECF, and self-reporting plants that express optical pH-sensitive sensor proteins. A detailed outline of these methods is beyond the scope of this study; the reader is referred to a number of excellent reviews describing their advantages and potential pitfalls (Martinière *et al.*, 2013; Geilfus, 2017). Results obtained with this diverse spectrum of techniques are remarkably homogenous; under unstressed conditions pH_c values are slightly alkaline ranging between 7.1 and 7.5 (Kurkdjian & Guern, 1989; Katsuhara *et al.*, 1997; Gout *et al.*, 2001; Moseyko & Feldman, 2001; Halperin *et al.*, 2003; Gao *et al.*, 2004; Schulte *et al.*, 2006; Martinière *et al.*, 2018). When a salt treatment was included pH_c was found to be unaffected by salinity in most of the studies (Katsuhara *et al.*, 1997; Halperin *et al.*, 2003; Schulte *et al.*, 2006; but see also Gao *et al.* (2004) for a salt-induced acidification). Apoplastic pH_a is in the moderately acidic range, and values typically range from *c.* 4.9 to 5.8 (for an overview on the older literature, see Felle (2001); an update is provided by Geilfus, 2017). Higher values (*c.* pH 6.3) were reported by Gao *et al.* (2004) on transgenic *Arabidopsis* expressing pHluorin, a GFP derivative directed to the apoplast. When pHluorin was directly anchored to the external face of the plasma membrane, pH_o in the root cortex was in the same range (*c.* pH 6.4; Martinière *et al.*, 2018). The bulk measurements indicate a ΔpH of 1.5 to 2 units across the plasma membrane; the method of Martinière *et al.* (2018) which allows a more precise measurement of the actual ΔpH across the membrane, renders values between 1.0 and 1.7, increasing with radial distance from the root surface.

The P-ATPases contribute to this pH gradient by sequestering H^+ from the cytosol into the apoplast (for a primer on the basics of membrane transport see e.g. Volkov, 2015). Proton pumping usually operates at a stoichiometry of *c.* 1 H^+ per ATP molecule split into ADP and P_i (even though this number can apparently be variable and increase to *c.* 3, e.g., under saline conditions; Janicka-Russak & Kłobus, 2007). Concomitantly, the export of positive charges leads to a hyperpolarization of the plasma membrane. The resulting electrochemical H^+ gradient fuels passive transport processes that exploit the H^+ concentration gradient (e.g. in case of the antiporter SOS1 that exchanges Na^+ in the cytosol for an equal amount of H^+; Qiu *et al.*, 2003), the membrane potential (e.g. in case of K^+ channels for low-affinity K^+ uptake; Wegner *et al.*, 1994), or both (which applies, e.g. to high-affinity K^+ uptake via KUP/HAK transporters that co-transport K^+ and H^+; Rodríguez-Navarro, 2000). An overview on transporters exploiting the ΔpH or the pmf across the plasma membrane for secondary active solute transport, either by cotransport or by antiport, is given in Table 1. It is generally believed that a circular H^+ flow across the membrane is established in the steady state with H^+ efflux via the proton pump being compensated by H^+ influx via transporters that take advantage of the driving force generated by the pump, for example, for nutrient uptake. If required, charge balance may be achieved via ion channels. According to this rationale, blocking of the secondary transport processes would also terminate proton pump activity within a short time, and *vice versa* (Felle, 2001).

However, this tight balance of H^+ uptake and release, leading to zero net H^+ flux across the plasma membrane under steady state conditions, is frequently not confirmed experimentally. Detailed studies have been performed using noninvasive ion flux monitoring with microelectrodes on roots under hydroponic conditions (Newman, 2001; commercialized as microelectrode ion flux estimation (MIFE) or scanning ion-selective electrode technique (SIET)). The absolute values of H^+ fluxes obtained on plant tissues have to be interpreted with some care because of the unknown buffering effects of the cell wall, but tendencies are reliable (Arif *et al.*, 1995). Fig. 1(a) shows an example of prolonged (< 2 h) net H^+ influx recorded on the elongation zone of a maize root, *c.* 5 mm away from the root tip. The root was immersed in a dilute electrolyte solution (pH 4.0). Oscillatory patterns with a phase length of 7 to 10 min reflect changes in proton pump activity; they are superimposed on a slowly decreasing H^+ influx. Net H^+ influx was also observed in similar recordings on roots of numerous other species, including *Arabidopsis* (Shabala *et al.*, 2005), poplar (Sun *et al.*, 2009; Luo *et al.*, 2013), soybean, Douglas fir (Hawkins & Robbins, 2010), cotton (Kong *et al.*, 2012) and *Nitraria sibirica* (Tang *et al.*, 2018). It ranges from 10 to 1200 nmol m^{-2} s^{-1}. This is at variance with the model of exclusively H^+ ATPase-driven transport processes outlined earlier. For a net H^+ influx measured on complex organs like roots it could be argued that microelectrode techniques can only record local fluxes. Thus, H^+ influx measured this way may just pass through a number of cells (or around them, through the apoplast) and may be compensated by H^+ efflux at another site, giving rise to circular currents passing through the organ (Weisenseel *et al.*, 1979). Indeed, H^+ fluxes can be patchy, and tend to vary strongly with distance from the apex. For instance,

Table 1 Plasma membrane-located transporters that rely on a ΔpH, or on the proton motive force (pmf).

Acronym	Substrate (beside H^+)	Classification	Driving force	Stoichiometry	Selected literature
SOS1	Na^+	Antiporter	ΔpH	$1H^+$:$1Na^+$	Qiu *et al*. (2003)
CHX13,17,21	Na^+, K^+, . . .?	Antiporter	ΔpH	$1H^+$:1 cation	Chanroj *et al*. (2012)
CAX1	Ca^{2+}	Antiporter	pmf	$1H^+$:$1Ca^{2+}$	Luo *et al*. (2005)
BOR	Borate	Antiporter	pmf	?	Hayes & Reid (2004)
PHT.1	Phosphate	Cotransporter	pmf	2-4H+:$1H_2PO_4^-$	Ullrich-Eberius *et al*. (1981)
KT/KUP/HAK (HAK5)	K^+	Cotransporter	pmf	$1H^+$:$1K^+$	Rodríguez-Navarro (2000)
NRT1	Nitrate	Cotransporter	pmf	$2H^+$:$1NO_3^-$	McClure *et al*. (1990)
NRT2.1					
SULTR1	Sulphate	Cotransporter	pmf	$3H^+$:$1SO_4^{2-}$	Lass & Ullrich-Eberius (1984), Hawkesford *et al*. (1993)
NRAMP	Metal ions	Cotransporter	pmf	?	Thomine & Schroeder (2013)
ZmYS1	Chelated divalent metals (Fe^{2+}, Zn^{2+}, Cu^{2+})	Cotransporter	pmf	?	Schaaf *et al*. (2004)
SUT	Sucrose	Cotransporter	pmf	$1H^+$:1 sucrose	Boorer *et al*. (1996)
AAP1-6	Amino acids	Cotransporter	pmf	$1H^+$:1 amino acid	Fischer *et al*. (2002)
LHT	Amino acids (lysine, histidine)	Cotransporter	pmf	?	Chen & Bush (1997)
ProT	Proline	Cotransporter	pmf	?	Ueda *et al*. (2001)
AUX1/LAX	Auxine	Cotransporter	pmf	?	Lomax *et al*. (1985), Yang *et al*. (2006)

H^+ efflux occurs in the elongation zone, and net influx in the mature zone (Newman, 2001), or H^+ entry is confined to the tip and H^+ efflux to the elongating zone (Rao *et al.*, 2002). However, under some conditions this pattern could be manipulated in such a way that independent of the axial position along the root only H^+ influx was observed (e.g. with soybean roots at an external pH of 4.0; Hawkins & Robbins (2010), and with poplar roots under saline conditions; Sun *et al.*, 2009), providing evidence for a true imbalance of H^+ fluxes for this organ. Moreover, a continuous net H^+ influx was also observed for example with protoplasts, that potentially render more accurate flux values due to the absence of a cell wall (see earlier). Fig. 1(b) shows net H^+ fluxes that were recorded simultaneously on opposite poles of a protoplast derived from maize coleoptile. The magnitude of the fluxes differed somewhat, providing evidence for a weak flux polarity (Shabala *et al.*, 1998), but a net influx was observed on both sides, indicating continuous H^+ uptake for > 1 h. Shabala & Newman (2000) also documented net H^+ influx for a protoplast isolated from bean leaf protoplast. In that case H^+ flux was only recorded at one side, but the possibility that H^+ influx was balanced by a pump-driven H^+ efflux opposite to the site of measurement was precluded by adding the ATPase blocker *ortho*-vanadate to the bath.

These observations can only be explained by a continuous buffering of pH changes induced by the H^+ flux. (Theoretically, H^+ influx could also be driven by the substrate to which its translocation is coupled, either by cotransport or by antiport. However, in the experiments reported earlier no substrate with an adequate gradient in free energy could be identified. Moreover, the problem of continuous acidification of the cytosol would remain.) Thus, H^+ influx tends to acidify the cytosol and to alkalinize the apoplast, but by effective intracellular and extracellular buffer systems relying on metabolism (to be discussed in detail later) both effects could be mitigated and the ΔpH across the membrane be maintained. Sakano (2001) argued that relying on H^+ gradients (or, rather, the pmf) as a primary energy source for driving membrane transport was evolutionary favorable for a sessile life form on land (compared to a system based on Na^+/K^+ gradients as found in animals), since H^+ can be generated (and annihilated) without the need for an external source of this ion (see also Raven, 1986). Consistently, when studying phosphate uptake via a cotransport with H^+ on P starved culture cells, Sakano *et al.* (1992) reported that the cytosol started to acidify shortly after addition of phosphate but ceased soon despite ongoing, H^+ driven phosphate influx, as reflected by the gradual increase in *apoplastic* pH. The latter indicated that the proton pump was apparently insufficient to balance this H^+ influx and, hence, a pH stat mechanism was operating in the cytosol.

If buffering effects contributed significantly to the energization of the plasma membrane, this should become manifest when the proton pump is blocked by a specific inhibitor, for example, by applying *ortho*-vanadate. In poplar roots supplied with NO_3^- and/or NH_4^+ as nitrogen (N) source, net H^+ efflux turned to steady influx after blocking ATPases, or initially low H^+ influx increased considerably (Luo *et al.*, 2013). This is consistent with a loss of H^+ efflux mediated by the H^+ ATPase. Interestingly, uptake of nitrate continued in the presence of the P-ATPase inhibitor, albeit at a reduced rate. In protoplasts derived from bean leaf mesophyll, H^+ influx also increased upon administration of vanadate (Shabala & Newman, 2000). Subsequent exposure to 90 mM sodium chloride (NaCl) induced a further increase in H^+ influx. Other studies confirmed H^+-driven influx to continue at a reduced level upon addition of the blocker. Phosphate uptake into maize root tips decreased by *c.* 40% in the presence of 1 mM Na-vanadate with respect to controls (Sklenar *et al.*, 1994). Thibaud *et al.* (1988) observed a similar reduction of P_i influx into corn roots by addition of 0.2 mM vanadate at an external pH of 5.8. When the pH was increased to 7.2 in the presence of the inhibitor, P_i uptake was completely blocked. Interestingly, vanadate had only a minor effect on the apoplastic pH (*c.* 0.2 units increase upon 4 h-exposure to 0.5 mM Na-vanadate in pea and lupin roots; Yu *et al.*, 1999) and

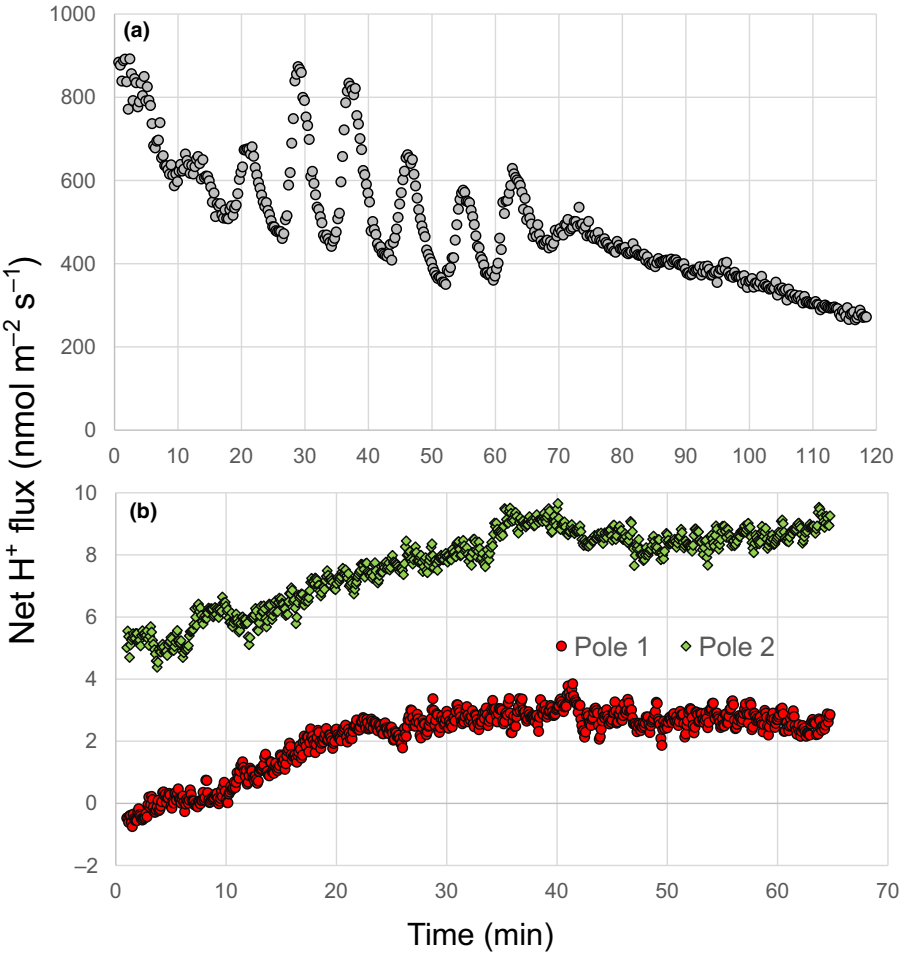

Fig. 1 Examples of prolonged net H^+ fluxes measured on various plant tissues. (a) Net H^+ fluxes recorded on the epidermal cells of maize (*Zea mays* cv Aussie Gold) root in the middle of the elongation zone (5 mm from tip) using noninvasive microelectrode ion flux estimation (MIFE) technique. Bath solution was 0.2 mM $CaSO_4$; 0.5 mM KCl; pH 4.0 (unbuffered). One typical example out of seven experiments is shown. The sign convention is 'influx positive'. Fast (ultradian) oscillations between 10 and 70 min are associated with root nutation (e.g. Shabala & Newman, 1997). (b) Net H^+ fluxes measured from two opposite poles of a protoplast isolated from 5-d old maize (*Zea mays* cv Aussie Gold) coleoptiles. Protoplasts were isolated using an enzymatic digestion method as described in Shabala *et al*. (1998). The measuring solution was 0.1 mM $CaCl_2$, 0.1 mM KCl, 0.6 M mannitol, pH 5.9. One typical example out of 12 experiments is shown. The theory of MIFE noninvasive ion flux measurements and full details of H^+ microelectrodes manufacturing and calibration are available from our previous publications (Shabala & Newman, 1997; Shabala *et al*., 2005).

did not affect cytosolic pH, in contrast to inhibitors of respiration like cyanide and DCCD that induced a significant acidification (Felle, 2001). The latter would also impair the biochemical pH clamp. As shown in the next section, the passive buffer capacity of the cytosol and the apoplast could only transiently alleviate pH changes by net H^+ fluxes across the membrane with no ATPase activity. Hence, some active buffering of H^+ coupled to metabolism has to be postulated, with H^+ being continuously generated and consumed in the apoplast and in the cytosol, respectively.

Here, the problem of charge balance associated with net H^+ fluxes across the membrane needs some extra attention. Buffering can prevent a breakdown of the trans-membrane H^+ concentration gradient, but *not* the associated depolarization by influx of positive charge. Therefore, unless H^+ influx drives a transport process that is, *in summa*, electroneutral, an electrogenic transport is additionally required to maintain charge balance during active pH buffering. By contrast, the proton pump can compensate for both the changes in H^+ concentration and the import of positive charges induced by H^+ influx. Consider, for example, RTSC driven by the proton pump (Fig. 2a) and by active buffering (Fig. 2b). Here, Na^+ influx via nonselective cation channels (NSCCs) is followed by salt overly sensitive 1 (SOS1)-mediated back-transport into the apoplast which is driven by a H^+ influx. According to the scenario shown in Fig. 2(a), the underlying H^+ gradient is provided by the proton pump which compensates, at the same time, for charge influx by Na^+. If RTSC is driven by active buffering instead (Fig. 2b), charge balance is not achieved, and K^+ efflux (Sakano *et al*., 1992) and/or anion influx are additionally required to maintain electroneutrality. Hence, K^+ loss would indeed be detrimental for the plant in the long run, given that the estimated buffering capacity of vacuolar K^+ does not exceed 7 h (Wu *et al*., 2018). Alternatively, when cells are sufficiently depolarized, passive, channel-mediated uptake of chloride or nitrate may occur. In any case, electrically unbalanced H^+ influx associated with the

biochemical pH clamp short-circuits the proton pump and entails a membrane potential shift from the hyperpolarized 'pump-state' to values more positive than the Nernst potential of potassium.

The mechanism depicted in Fig. 2(b) is supported by the observation that salt treatment tends to increase net H^+ influx at least transiently, for example, in poplar root (Sun *et al.*, 2009), which is consistent with a release of Na^+ via antiport with H^+ to counterbalance NSCC-mediated Na^+ influx into the cytosol. Salinity also stimulated net H^+ influx into root protoplasts derived from poplar roots.

Biochemical mechanisms of active pH buffering in respiring cells

As mentioned earlier, passive buffering refers to the buffer capacity of the cytosol and the apoplast. The cytosolic buffer capacity usually given in mM per pH unit has been determined for a range of cell types and species; values of 20 to 80 mM/ΔpH were found in the physiologically relevant cytosolic pH range (pH 7–8; Kurkdjian & Guern, 1989; Felle, 2001). It is due to (oligo)phosphates as well as various macromolecules with weakly acidic or basic groups. Cell wall pK (*c.* 3.2) is dominated by pectins consisting, to a large part, of polygalacturonic acids (Grignon & Sentenac, 1991). The apoplastic buffer capacity is supposed to amount to about one tenth of the cytosolic one, critically depending on the degree of methylation of the carboxyl groups. It is clear that the passive buffer capacity of both compartments will soon be exhausted (in the range of minutes up to about an hour, depending on the proton influx, and the tolerable pH deviation; see Raven, 1985, 1986). Moreover, after this time period it would have to be restored by H^+ efflux before becoming functional again. Surplus H^+ could also be disposed in the vacuole (Raven & Smith, 1976; Smith & Raven, 1979); this compartment has a much larger volume (but also a lower buffer capacity) than the cytosol. Vacuolar H^+ sequestration does not rely on the V-ATPase alone. It is additionally driven by the ATP-independent pyrophosphatase, which would be an advantage when ATP is limiting. However, due to the limited buffer capacity of the vacuolar sap, H^+ pumping into the vacuole can only transiently alleviate acidification of the cytosol. Therefore, mechanisms for long-term pH adjustment are required that take advantage of continuous metabolic proton consumption and generation in the cytosol and the apoplast, respectively.

A biochemical pH stat for pH fine tuning based on the cytosolic malate pool has been already suggested in the 1970s (reviewed in Davies, 1986). Carboxylation of phosphoenolpyruvate (PEP carboxylase) leading to the formation of oxaloacetate, which is subsequently oxidized to malate, is proposed to generate H^+ in order to reverse alkalinization of the cytosol. Acidification, however, is counteracted by malic enzyme, forming pyruvate from malate. Consistently, both enzymes are characterized by strongly opposing pH dependencies; PEP carboxylase is activated by an alkalinization of the cytosol, whereas acidification favors malate breakdown by the malic enzyme. One H^+ is captured by decarboxylation of malate and formation of CO_2. Sakano (1998) stressed that the reaction catalyzed by malic enzyme does not involve net H^+ consumption due to the simultaneous reduction of NAD(P)+ to NAD(P)H+ H^+. Arguably, the latter reaction step does not affect cytosolic pH at a constant cytosolic redox state, though, and it is an academic question if cytosolic alkalinization is brought about by the malic enzyme itself, or rather by subsequent oxidative phosphorylation (Sakano, 1998; see also Fig. 3a). Impressive evidence in favor of malate decarboxylation and subsequent reactions operating as a H^+ scavenger was obtained on *Acer pseudoplatanus* culture cells (Mathieu *et al.*, 1986). Exposure to weak acids that traverse the plasma membrane induced a transient acidification of the cytosol; subsequent pH recovery (still in the presence of the acid) was correlated with an *c.* 30% loss of stored malate. Malate decarboxylation accounted for *c.* 40% of the pH recovery; the residual part was ascribed, at least partly, to the proton pump. However, when malate is generated from *glucose* before decarboxylation, it is associated with the release of $4H^+$. Hence, decarboxylation of malate derived from glycolysis is unsuitable for capturing H^+ ions imported via the plasma membrane (Sakano, 1998, 2001), and malate previously stored

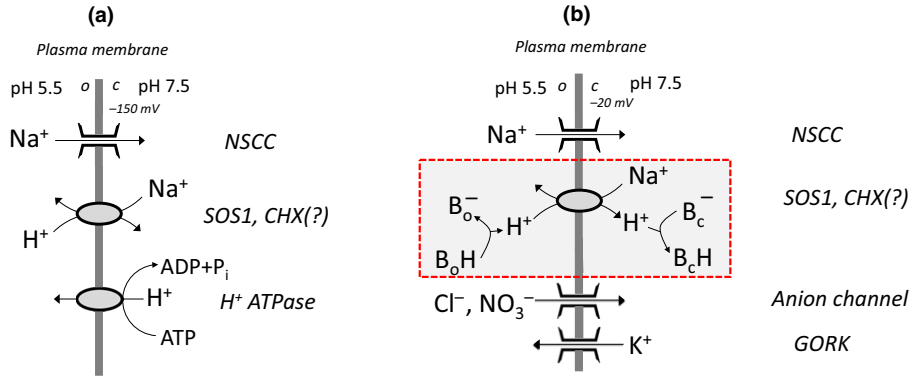

Fig. 2 Ion fluxes under saline conditions in root epidermal and cortex cells. (a) The current state of knowledge is shown (cf. Munns *et al.*, 2019) with transport processes across the plasma membrane ('o' outside, 'c' cytosol) supposed to be fueled by the P-type ATPase. The cell is in a hyperpolarized state (membrane potential −150 mV). By contrast, (b) illustrates a case without proton pump activity. Here, Na^+-H^+ antiport is driven by active buffer systems (red box; B_o and B_c in the apoplast and in the cytosol, respectively) that sustain the pH gradient across the membrane despite H^+ influx. The cell is in a depolarized state (−20 mV). Charge balance is maintained by K^+ efflux and/or NO_3^- or Cl^- influx mediated by ion channels. GORC, guard cell outward rectifying K(+) channel; NSCC, nonselective cation channel; SOS1, salt overly sensitive 1; GHX, cation:proton antiporter.

in the vacuole is required (as in the case of the *Acer* culture cells). Alternatively, root cells import malate from the shoot via the phloem as proposed by the Ben-Zioni Lips model (BenZioni *et al.*, 1971; Fig. 3a). According to this model, potassium nitrate (KNO_3) is exported from the root to the shoot, the preferred site of nitrate assimilation in many species. Thus, K^+ is subsequently recycled back to the root using malate^{2-} as a counterion (at the same time, H^+ formation during malate synthesis serves as a remedy for the alkalinization by nitrate assimilation; Raven & Smith, 1976). Furthermore, K_2 malate may diffuse via a symplastic pathway from the phloem into root cells. In fact, metabolic decomposition of malate in the way described here was already anticipated by BenZioni *et al.* (1971). The model was confirmed experimentally for some plant species including soybean (Touraine *et al.*, 1992), but results were less conclusive, for example, for *Ricinus* (Allen & Raven, 1987; Peuke *et al.*, 1996), indicating that it may operate species-dependent, and not under all physiological conditions (obviously, it is limited to the use of nitrate as an N source, and nitrate assimilation in the leaves). Interestingly, formation of pyruvate favors the activation of the alternative oxidase which catalyzes electron transfer to oxygen, without any ATP synthesis (Day *et al.*, 1994). The physiological role of the alternative pathway of respiration is an intensely debated issue (Millenaar & Lambers, 2003; Munns *et al.*, 2019). It is an apparent paradox that this pathway is favored under conditions of stress (e.g. with salinity), when there is an extra need for metabolic energy (Munns *et al.*, 2019). In the framework of the model proposed here, the alternative oxidase is part of a machinery to allocate metabolic energy exclusively to the plasma membrane by annihilating protons that enter the cytosol (and favoring H^+ formation in the apoplast, see later), thus stabilizing the trans-membrane pH gradient. A hitherto undiscovered link between metabolism and membrane transport is proposed here, in addition to the 'common' link via ATP synthesis by oxidative phosphorylation providing the substrate for the proton pump. However, the ATP pool has to be shared with competitive energy consumers, that is growth and maintenance (Poorter *et al.*, 1991). Hence, prioritization of energy allocation to the plasma membrane may be a problem under stress conditions (e.g. salinity) when ATP is the only energy source for membrane transport. At the same time, the alternative oxidase guarantees fast turnover rates in the upstream metabolism which is crucial for the biochemical pH clamp mechanism suggested here (see later).

Another metabolic pathway that is highly stimulated at various stress conditions and consuming H^+ is the so-called GABA shunt (Fig. 3b). GABA, or 4-aminobutyric acid, is a zwitterionic, nonprotein amino acid that is found in almost all plants species and tissues. It is produced via an anaplerotic pathway branching from the tricarboxylic acid (TCA) cycle that involves trans-amination of 2-oxoglutarate leading to the formation of glutamate, and subsequent decarboxylation. The latter reaction is catalyzed by the glutamate decarboxylase (GAD) and consumes one H^+ ion (Fig. 3b). GABA can be fed back into the TCA cycle by a two-step process yielding succinate; alternatively, it is released into the apoplast. The pivotal role of the GABA shunt in preventing acidification of the cytosol is known since the pioneering work of Crawford on carrot suspension cells (Crawford *et al.*, 1994) who discussed GABA formation rather in the context of cytosolic pH regulation, than with respect to the energization of the plasma membrane. Interestingly, cytosolic acidification stimulates the GAD, and, in turn, GABA formation (Crawford *et al.*, 1994; Carroll *et al.*, 1994; for a review, see Shelp *et al.*, 1999). GABA concentrations in the cytosol can be as high as 6–39 mM under stress conditions such as drought stress and salinity (see also Renault *et al.*, 2010). A recent study by Che-Othman *et al.* (2019) revealed that in wheat leaves suffering from salinity the GABA shunt is strongly preferred over the alternative route via the 2-oxoglutarate dehydrogenase complex (OGDC) that forms part of the TCA cycle. The OGDC complex is disintegrated by elevated cytosolic NaCl concentrations, whereas expression of GABA shunt enzymes is strongly enhanced. It should be noted that H^+ is scavenged by GAD at the expense of 1 GTP formed by the alternative processing of 2-oxoglutarate via the TCA cycle. Ammonium assimilation was also shown to induce a mild cytosolic acidification and, at the same time, a stimulation of the GABA shunt (Carroll *et al.*, 1994). The role of the GABA shunt in facilitating H^+ driven membrane transport was indirectly shown by Snedden *et al.* (1992) who fed radioactively labeled glutamate to isolated *Asparagus* mesophyll cells. Glutamate uptake via symport with H^+ led to a progressive alkalinization of the apoplast (that could apparently not be fully compensated by the proton pump), and to GABA formation. The pH optimum of the GAD was found to be at *c.* 6, far outside the range that usually prevails in the cytosol of plant cells, but in line with an activation of that enzyme by cytosolic acidification. GABA itself appears to have multiple signaling functions, in analogy to its role as a neurotransmitter in animal cells (Ramesh *et al.*, 2017); when released into the apoplast, GABA controls the activity of anion channels of the ALMT type.

Carbon dioxide (CO_2) released by the decarboxylation reactions as described earlier gives rise to the formation of bicarbonate (with H_2CO_3 as an intermediate) at cytosolic pH. This reaction compromises cytosolic active buffering, since one H^+ is produced during this reaction, thus reversing previous H^+ consumption. Note that the equilibrium is strongly on the side of the bicarbonate at the usual pH_c values above 7. This aspect is usually ignored in discussion of cytosolic pH stats; Raven & Newman (1994) calculated rates of 0.063 mol HCO_3^- m^{-3} s^{-1} and up to 0.185 mol HCO_3^- m^{-3} s^{-1} for the generation of bicarbonate from CO_2 formed during respiration (taking into account that the reaction is spontaneous, but relatively slow), but these values may be overrated, at least in roots, for the following two reasons: (1) Membrane permeability is much higher for CO_2 than for HCO_3^-, and, hence, CO_2 will diffuse more readily out of the cell into the apoplast, leading to an up-concentration of intracellular HCO_3^- (that is consumed at low rates only by root metabolism) even without any chemical conversion. (2) Intracellular activity of carbonic anhydrase (CA), the enzyme that could speed up bicarbonate formation, is associated with organelles (plastids, mitochondria; DiMario *et al.*, 2017), and seems to be largely absent from the cytosol whereas GAD and NADP-dependent malic enzyme are cytosolic enzymes. Consistently, CO_2 is constantly released from respiring roots, as expressed by a 'respiratory

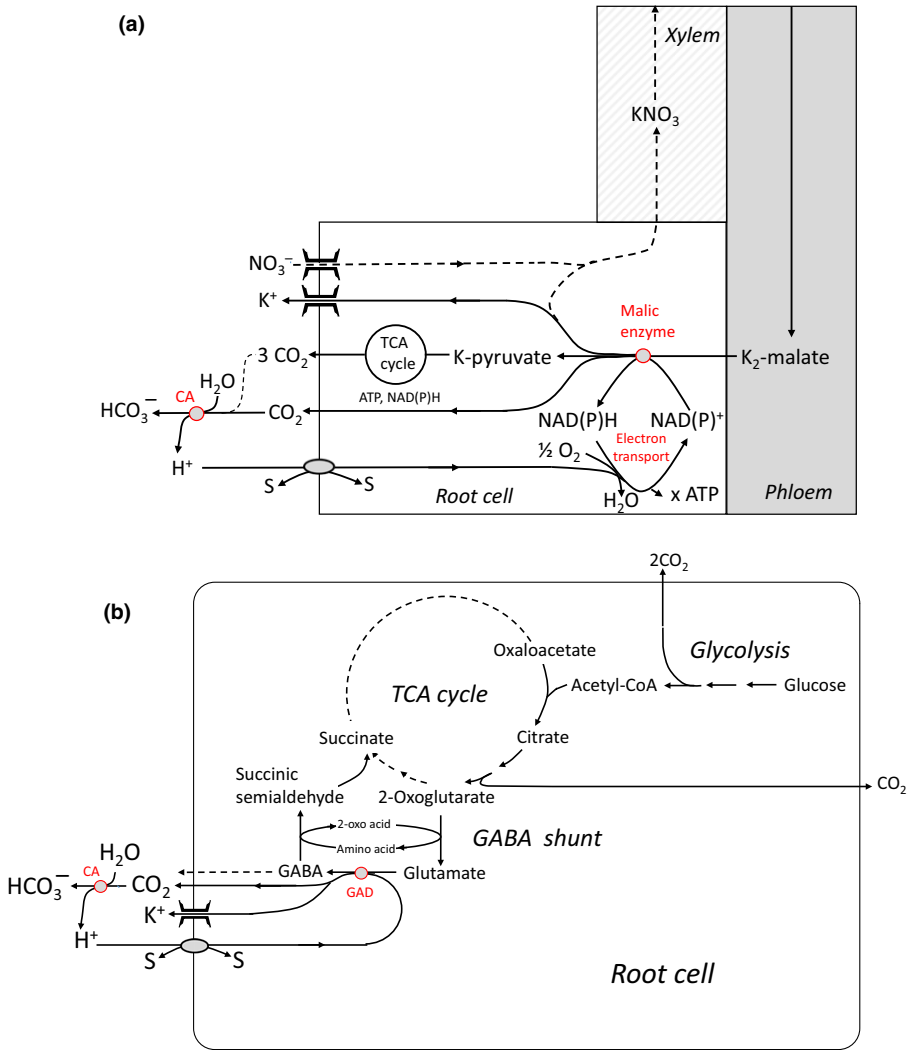

Fig. 3 Metabolic schemes showing 'active' buffering in the cytosol by malic enzyme and the electron transport chain (a) and the glutamate decarboxylase (GAD) which is part of the GABA shunt (b). Both systems are capable of capturing H^+ imported by cotransport with or antiport against other substrates ('s'). Extracellular buffering is brought about by the carbonic anhydrase (CA). For more details, see text.

quotient' (RQ) that relates CO_2 release (in its gaseous form!) to oxygen (O_2) uptake (Lambers *et al.*, 1996). The theoretical RQ value of 1 calculated from the stoichiometry of respiration with sugars as a substrate is indeed frequently measured on young tissues. Even higher values are obtained, for example, when malate is metabolized (for more details, see Lambers *et al.*, 1996). Intracellular conversion of CO_2 to HCO_3^- is apparently of minor importance for this ratio (and the same is true for extracellular bicarbonate formation, at least at a pH < 6, see later), suggesting that decarboxylation of malate and glutamate is indeed associated with a net consumption of H^+.

The anaplerotic GABA shunt also links energy metabolism with N assimilation. In fact, the earlier considerations on the cytosolic part of the biochemical pH clamp would be incomplete without considering nitrate and ammonium assimilation that are known to have a strong effect on cytosolic pH. Nitrate assimilation is usually thought to result in the formation of $2OH^-$ per nitrate being reduced to NH_4^+, and cytosolic alkalinization is counter-acted by H^+ formed during malate synthesis (Raven & Smith, 1976; Smith & Raven, 1979). Later, this scheme was critically reviewed by Britto & Kronzucker (2005). They took membrane transport processes and synthesis of the carbon-skeletons of amino acids (in that case, glutamate), starting from glucose, into account (the rationale being that neither NH_3 nor NH_4^+ are preferred forms of N storage and transport and, hence, nitrate assimilation directly leads to amino acid synthesis). It was argued that the uptake of each nitrate molecule goes with the net transfer of one H^+ from the apoplast into the symplast to maintain charge balance (or, rather, $1H^+$ is released into the apoplast by the proton pump, while $1NO_3^-$ is taken up via cotransport with $2H^+$; McClure *et al.*, 1990). Nitrate reduction to ammonium and subsequent glutamate synthesis would *in summa* be 'H^+-neutral'. Hence, Britto & Kronzucker (2005) came to the conclusion that nitrate assimilation tends to acidify the cytosol (one H^+ surplus per N assimilated if glutamate is the end product), whereas the apoplast is alkalinized. One is left with the conclusion that nitrate uptake and subsequent assimilation cannot rely on the proton pump alone, but definitely requires an additional biochemical pH clamp system for avoiding progressive acidification of the

cytosol (even though no detailed mechanism was suggested by Britto & Kronzucker, 2005). For nitrate uptake driven by the biochemical pH clamp alone (with no proton pump involved) net H^+ influx would even be twice the influx of nitrate, potentially accelerating the alkalinization of the rhizosphere.

According to Britto & Kronzucker (2005), amino acid synthesis with ammonium serving as N source is acidifying both the cytosol (in agreement with previous studies; Raven, 1985; Carroll *et al.*, 1994), and the apoplast (Allen & Allen, 1987).

Even though a fully comprehensive analysis of the cytosolic part of the biochemical pH clamp system would have to include S assimilation and secondary metabolism as well, this is not attempted here because of the enormous complexity of the multiple metabolic pathways and their cell-specific variability. The reader is referred to earlier approaches by Raven (1986) and Sakano (2001).

So far, the discussion on biochemical mechanisms has centered on pH control in the cytosol. However, adjustment of the *apoplastic* pH is equally important for sustaining H^+ influx into cells, since H^+ ions have to be generated there at about a constant rate. Even though the buffer capacity of the cell wall is much lower compared to the cytosol, pH is known to be regulated tightly, at least under unstressed conditions (Peters & Felle, 1991; Felle, 1998; Martinière *et al.*, 2018). However, under conditions of large H^+ influx, for example under salinity, and at high rates of phosphate uptake, the pH can shift (Sakano *et al.*, 1992; Gao *et al.*, 2004), for example from values of *c.* 5.5 to above 6 (indicating that we are dealing with a rather loose pH clamp which allows some variation of the H^+ gradient mostly originating on the apoplastic side). It has to be kept in mind, though, that under natural conditions the root apoplast is in contact with the soil solution that serves as an 'infinite' buffer system, and source of H^+. Consistently, H^+ moving into the cell is partly replenished by H^+ invading from adjacent soil layers (or release of OH^- by the root into the soil). This leads to a progressive alkalinization of the rhizosphere correlating with nitrate and/or phosphate uptake (Hinsinger *et al.*, 2002). Furthermore, H^+ released by the apoplastic CO_2/HCO_3^- -buffer system plays an important role (Fig. 3a,b). With a pK value of 6.35, it is largely irrelevant when the pH is below 6, but when the pH increases beyond that level, bicarbonate is formed from respiratory CO_2 that diffuses from the cytoplasm into the apoplast (see earlier). The reaction is facilitated by the CA. So far, the activity of *apoplastic* CA was mostly studied on submerged aquatic plants, for example, on *Ranunculus penicillatus* ssp. *pseudofluitans* (Newman & Raven, 1993). CA associated with the cell wall was also found in rice culture cells (Chen *et al.*, 2009), and it is proposed here to play an important role for producing H^+ at elevated apoplastic pH values and, hence, in the apoplastic part of the biochemcial pH clamp. It seems likely that other apoplastic biochemical reactions yet to be identified are also involved in the apoplastic H^+ control. Our knowledge of the extracellular enzyme spectrum is still incomplete.

The biochemical pH clamp: thermodynamic and energetic aspects

The last part of this Viewpoint is dedicated to a quantitative, thermodynamic treatment of the hypothesis outlined earlier.

In a steady state situation, with a constant cytosolic pH, net H^+ influx ($J^{net}_{H+,in}$) across the plasma membrane corresponds to the sum of carrier-mediated H^+ influx ($J_{H+,c}$), and efflux catalyzed by the P-type ATPase ($J_{H+,p}$, with a negative sign). This net flux is equal to the (hypothetical) decrease in the cytosolic H^+ concentration brought about by biochemical H^+ capturing ($d[H^+]_{cyt}/dt$) due to malate and/or glutamate decarboxylation (passive buffering is irrelevant for the H^+ balance under steady state conditions), times a factor that relates cytosolic volume (V_{cyt}) to cell surface (A), assuming homogenous concentrations throughout the cytosol. Proton consumption, in turn, can be related to the carbon flux through the metabolic pathway(s), which is approximately equal to the CO_2 efflux from the cells (J_{CO_2} in mol m^{-2} s^{-1}, with a negative sign). A stoichiometric factor ν is introduced counting the number of protons that are captured per released CO_2.

$$J^{net}_{H+,in} = J_{H+,c} + J_{H+,ATPase} = -\frac{d[H^+]_{cyt}}{dt}\frac{V_{cyt}}{A} = -\nu J_{CO_2}. \quad \text{Eqn 1}$$

For the apoplast we can write:

$$J^{net}_{H+,out} = -J^{net}_{H+,in} = -J_{H+,c} - J_{H+,ATPase}. \quad \text{Eqn 2}$$

Thus, H^+ uptake follows the pmf across the plasma membrane. The free energy released per time increment (that can be utilized for the accumulation of other solutes by cotransport or antiport, compare Table 1) is described by:

$$\frac{dG_{H+,in}}{dt} = J_{H+,c} \times A \times (2.303 \times RT(pH_{apo} - pH_c) + F \times \Delta E_M), \quad \text{Eqn 3}$$

With R, T and F being the gas constant, the absolute temperature and the Faraday constant, respectively, and ΔE_M is the membrane potential of the cell. Eqn 3 is equal to the rate of free energy loss by the cell due to H^+ influx. So far, ATP hydrolysis by the ATPase was considered to be the only source of energy to drive this process and provide the necessary energy (Wegner, 2015). As shown here, metabolic energy can also be invested into the biochemical pH clamp to maintain the pH gradient:

$$\frac{dG_{\Delta pH}}{dt} = J^{net}_{H+,in} \times A \times (2.303 \times RT(pH_c - pH_{apo})). \quad \text{Eqn 4}$$

Note that $J^{net}_{H+,in}$ is equal to H^+ influx not supported by the proton pump (see earlier; note further that the contribution of ΔE_M to H^+ flux is ignored in Eqn 4)! This input results from the free energy loss by the metabolic pathway(s) that are involved in capturing H^+ in the cytosol (and partly generating H^+ in the apoplast). The use of Eqn 4 implies that the membrane potential is stabilized during H^+ influx, for example by K^+ efflux (otherwise H^+ influx would only be transient, see earlier). Malate decarboxylation is energetically slightly uphill under standard conditions (Li *et al.*, 2010) and, by itself, is no reliable source of energy. However, subsequent oxidation of the product NAD(P)H is a strongly

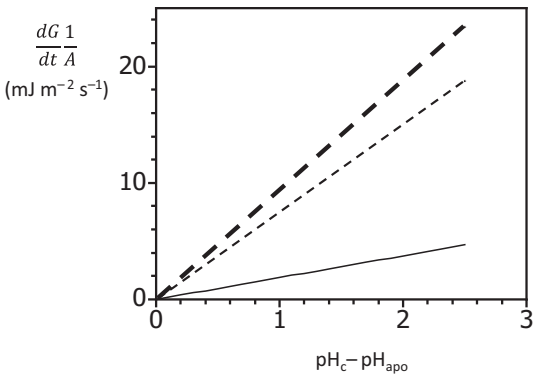

Fig. 4 Energetic cost of H^+ influx following the pH gradient across the plasma membrane (cytosolic pH – apoplastic pH), as decribed by Eqn 4. The electrical force is not considered. Data for net H^+ influx were taken from an experiment on a bean mesophyll protoplast shown by Shabala & Newman (2000; their Fig. 1c). Energy costs as a function of ΔpH (not determined for this experiment) for H^+ influx under control conditions (thin continuous line) and for the increase in flux after addition of vanadate (thin dotted line). The latter is supposed to represent the free energy consumed by the proton pump under control conditions to drive H^+ influx. The sum of both (thick dotted line) corresponds to the total free energy invested into active buffering in the presence of the inhibitor.

downhill reaction provided that the alternative respiration pathway is involved. Respiration via cytochrome *c*, by contrast, is associated with little free energy release that may be insufficient for sustaining the biochemical pH clamp including the necessary energetic 'safety margin'. In fact, this could be the reason why the alternative respiratory pathway as well as uncoupling proteins (UCPs; Pu *et al.*, 2015) become more prominent under stress conditions, when additional energy has to be allocated specifically to the plasma membrane. The second mechanism of H^+ consumption by decarboxylation of glutamate is also energetically downhill; Efe *et al.* (2008) calculated a free energy release of −35 to −17 kJ mol^{-1}, depending on the actual concentrations. It has to be stressed again that additional energy is required to balance the charge influx associated with H^+ uptake, either by release of previously accumulated K^+ stored in the vacuole, serving as a kind of 'battery' for plasma membrane transport, or by channel-mediated anion uptake (provided that anion concentrations are higher outside than inside the cell to overcome the negative membrane potential).

The contribution of the biochemical pH clamp to H^+-driven membrane transport can be estimated from measurements of H^+ fluxes with the MIFE technique, using Eqn 4 to calculate the free energy investment with time (Fig. 4). Measurements of net H^+ flux before and after addition of vanadate allow a tentative quantification of the contribution of the H^+ pump to the overall fluxes, based on the assumption that the biochemical pH clamp can fully compensate for the loss in transport capacity when the pump is blocked (at least transiently). This is supported by steady H^+ influx into roots in the presence of vanadate in the range of minutes to hours (Fig. 1; Shabala & Newman, 2000; Luo *et al.*, 2013). These experiments show that H^+ influx driven by the biochemical pH clamp can be roughly equal in size to pump-driven H^+ influx. However, the available data also suggest that under aerobic conditions, the biochemical pH clamp is rather an emergency mechanism that comes into play when the proton pump capacity is insufficient to maintain H^+-coupled solute influx which is vital for cell survival, for example Na^+ extrusion via SOS1 under saline conditions. For a more rigorous quantitative assessment of the biochemical pH clamp in different plant tissue types, simultaneous recordings of H^+ influx and the pH gradient across the plasma membrane (preferentially measured at the membrane surface) will be required. These data are not available yet. Moreover, the potential contribution of the biochemical pH clamp to membrane energization under extended periods of stress (e.g. salinity) is also not clear yet and requires further investigations.

Acknowledgements

The authors would like to thank Drs John A. Raven, Dundee, UK, and Vadim Volkov, Davis, CA, USA, for discussion, and for critical reading of an earlier version of the manuscript. SS received financial support from the China National Science Foundation (project 31870249).

ORCID

Sergey Shabala https://orcid.org/0000-0003-2345-8981
Lars H. Wegner https://orcid.org/0000-0002-9263-8436

Lars H. Wegner[1,2]* and Sergey Shabala[1]

[1]International Research Centre for Environmental Membrane Biology, Foshan University, Foshan, 528041, China;
[2] Present address: Hauptstraße 35, D-97892, Kreuzwertheim, Germany
(*Author for correspondence: tel +49 176 8169 8165; email lars.wegner@gmx.net)

References

Allen CR, Allen S. 1987. The titrimetric assay of H^+ excreted by *Ricinus communis* cultivated on NH^{4+}-N nutrient media: the effect of ionic strength and nutrient phosphate concentration. *Journal of Experimental Botany* **38**: 597–606.

Allen S, Raven JA. 1987. Intracellular pH regulation in *Ricinus communis* grown with ammonium or nitrate as N source: the role of long distance transport. *Journal of Experimental Botany* **38**: 580–596.

Arif I, Newman IA, Keenlyside N. 1995. Proton flux measurements from tissues in buffered solution. *Plant, Cell & Environment* **18**: 1319–1324.

BenZioni AB, Vaadia Y, Lips SH. 1971. Nitrate uptake by roots as regulated by nitrate reduction products of the shoot. *Physiologia Plantarum* **24**: 288–290.

Boorer KJ, Loo DDF, Frommer WB, Wright EM. 1996. Transport mechanism of the cloned potato H^+/Sucrose cotransporter StSUT1. *Journal of Biological Chemistry* **271**: 25139–25144.

Britto DT, Kronzucker HJ. 2005. Nitrogen acquisition, PEP carboxylase, and cellular pH homeostasis: new views on old paradigms. *Plant, Cell & Environment* **28**: 1396–1409.

Britto DT, Kronzucker HJ. 2015. Sodium efflux in plant roots: what do we really know? *Journal of Plant Physiology* **186–187**: 1–12.

Byrt CS, Zhao M, Kourghi M, Bose J, Henderson SW, Qiu J, Gilliham M, Schultz C, Schwarz M, Ramesh SA *et al.* 2017. Non-selective cation channel activity of

aquaporin AtPIP2;1 regulated by Ca^{2+} and pH. *Plant, Cell & Environment* **40**: 802–815.

Carroll AD, Fox GG, Laurie S, Phillips R, Ratcliffe RG, Stewart GR. 1994. Ammonium assimilation and the role of [gamma]-Aminobutyric acid in pH homeostasis in carrot cell suspensions. *Plant Physiology* **106**: 513–520.

Chanroj S, Wang G, Venema K, Zhang MW, Delwiche CF, Sze H. 2012. Conserved and diversified gene families of monovalent cation/H^+ antiporters from algae to flowering plants. *Frontiers in Plant Science* **3**: 25.

Chen L, Bush DR. 1997. LHT1, A lysine- and histidine-specific amino acid transporter in *Arabidopsis*. *Plant Physiology* **115**: 1127–1134.

Chen X-Y, Kim ST, Cho WK, Rim Y, Kim S, Kim S-W, Kang KY, Park ZY, Kim J-Y. 2009. Proteomics of weakly bound cell wall proteins in rice calli. *Journal of Plant Physiology* **166**: 675–685.

Che-Othman MH, Jacoby RP, Millar AH, Taylor NL. 2019. Wheat mitochondrial respiration shifts from the tricarboxylic acid cycle to the GABA shunt under salt stress. *New Phytologist*. doi: 10.1111/nph.15713.

Crawford LA, Bown AW, Breitkreuz KE, Guinel FC. 1994. The synthesis of [gamma]-aminobutyric acid in response to treatments reducing cytosolic pH. *Plant Physiology* **104**: 865–871.

Davies DD. 1986. The fine control of cytosolic pH. *Physiologia Plantarum* **67**: 702–706.

Day DA, Millar AH, Wiskich JT, Whelan J. 1994. Regulation of alternative oxidase activity by pyruvate in soybean mitochondria. *Plant Physiology* **106**: 1421–1427.

DiMario RJ, Clayton H, Mukherjee A, Ludwig M, Moroney JV. 2017. Plant carbonic anhydrases: structures, locations, evolution, and physiological roles. *Molecular Plant* **10**: 30–46.

Efe C, Straathof AJJ, van der Wielen LAM. 2008. Options for biochemical production of 4-hydroxybutyrate and its lactone as a substitute for petrochemical production. *Biotechnology and Bioengineering* **99**: 1392–1406.

Felle HH. 1998. The apoplastic pH of the *Zea mays* root cortex as measured with pH-sensitive microelectrodes: aspects of regulation. *Journal of Experimental Botany* **49**: 987–995.

Felle HH. 2001. pH: signal and messenger in plant cells. *Plant Biology* **3**: 577–591.

Fischer W-N, Loo DDF, Koch W, Ludewig U, Boorer KJ, Tegeder M, Rentsch D, Wright EM, Frommer WB. 2002. Low and high affinity amino acid H^+-cotransporters for cellular import of neutral and charged amino acids. *The Plant Journal* **29**: 717–731.

Fricke W. 2015. The significance of water co-transport for sustaining transpirational water flow in plants: a quantitative approach. *Journal of Experimental Botany* **66**: 731–739.

Gao D, Knight MR, Trewavas AJ, Sattelmacher B, Plieth C. 2004. Self-reporting arabidopsis expressing pH and [Ca^{2+}] indicators unveil ion dynamics in the cytoplasm and in the apoplast under abiotic stress. *Plant Physiology* **134**: 898–908.

Geilfus C-M. 2017. The pH of the apoplast: dynamic factor with functional impact under stress. *Molecular Plant* **10**: 1371–1386.

Gout E, Boisson A-M, Aubert S, Douce R, Bligny R. 2001. Origin of the cytoplasmic pH changes during anaerobic stress in higher plant cells. Carbon-13 and phosphorous-31 nuclear magnetic resonance studies. *Plant Physiology* **125**: 912–925.

Greenway H, Armstrong W. 2018. Energy-crises in well-aerated and anoxic tissue: does tolerance require the same specific proteins and energy-efficient transport? *Functional Plant Biology* **45**: 877–894.

Grignon C, Sentenac H. 1991. PH and ionic conditions in the apoplast. *Annual Review of Plant Physiology and Plant Molecular Biology* **42**: 3–28.

Halperin SJ, Gilroy S, Lynch JP. 2003. Sodium chloride reduces growth and cytosolic calcium, but does not affect cytosolic pH, in root hairs of *Arabidopsis thaliana* L. *Journal of Experimental Botany* **54**: 1269–1280.

Hawkesford MJ, Davidian J-C, Grignon C. 1993. Sulphate/proton cotransport in plasma-membrane vesicles isolated from roots of *Brassica napus* L.: increased transport in membranes isolated from sulphur-starved plants. *Planta* **190**: 297–304.

Hawkins BJ, Robbins S. 2010. pH affects ammonium, nitrate and proton fluxes in the apical region of conifer and soybean roots. *Physiologia Plantarum* **138**: 238–247.

Hayes JE, Reid RJ. 2004. Boron tolerance in barley is mediated by efflux of boron from the roots. *Plant Physiology* **136**: 3376–3382.

Hinsinger P, Plassard C, Tang C, Jaillard B. 2002. Origins of root-mediated pH changes in the rhizosphere and their responses to environmental constraints: a review. *Plant and Soil* **248**: 43–59.

Janicka-Russak M, Kłobus G. 2007. Modification of plasma membrane and vacuolar H^+-ATPases in response to NaCl and ABA. *Journal of Plant Physiology* **164**: 295–302.

Katsuhara M, Yazaki Y, Sakano K, Kawasaki T. 1997. Intracellular pH and proton-transport in barley root cells under salt stress: *in vivo* ^{31}P-NMR study. *Plant and Cell Physiology* **38**: 155–160.

Kong X, Luo Z, Dong H, Eneji AE, Li W. 2012. Effects of non-uniform root zone salinity on water use, Na^+ recirculation, and Na^+ and H^+ flux in cotton. *Journal of Experimental Botany* **63**: 2105–2116.

Kurkdjian A, Guern J. 1989. Intracellular pH: measurement and importance in cell activity. *Annual Review of Plant Physiology and Plant Molecular Biology* **40**: 271–303.

Lambers H, Atkin OK, Millenaar FF. 1996. Respiratory patterns in roots in relation to their functioning. In: Waisel Y, Eshel A, Kafkafi U, eds. *Plant roots. The hidden half, 2nd edn*. New York, NY, USA: Marcel Dekker, 529–556.

Lass B, Ullrich-Eberius CI. 1984. Evidence for proton/sulfate cotransport and its kinetics in *Lemna gibba* G1. *Planta* **161**: 53–60.

Li X, Dash RK, Pradhan RK, Qi F, Thompson M, Vinnakota KC, Wu F, Yang F, Beard DA. 2010. A database of thermodynamic quantities for the reactions of glycolysis and the tricarboxylic acid cycle. *Journal of Physical Chemistry B* **114**: 16068–16082.

Lomax TL, Mehlhorn RJ, Briggs WR. 1985. Active auxin uptake by zucchini membrane vesicles: quantitation using ESR volume and delta pH determinations. *Proceedings of the National Academy of Sciences, USA* **82**: 6541–6545.

Luo G-Z, Wang H-W, Huang J, Tian A-G, Wang Y-J, Zhang J-S, Chen S-Y. 2005. A putative plasma membrane cation/proton antiporter from soybean confers salt tolerance in *Arabidopsis*. *Plant Molecular Biology* **59**: 809–820.

Luo J, Qin J, He F, Li H, Liu T, Polle A, Peng C, Luo Z-B. 2013. Net fluxes of ammonium and nitrate in association with H^+ fluxes in fine roots of *Populus popularis*. *Planta* **237**: 919–931.

Malagoli P, Britto DT, Schulze LM, Kronzucker HJ. 2008. Futile Na^+ cycling at the root plasma membrane in rice (*Oryza sativa* L.): kinetics, energetics, and relationship to salinity tolerance. *Journal of Experimental Botany* **59**: 4109–4117.

Martinière A, Desbrosses G, Sentenac H, Paris N. 2013. Development and properties of genetically encoded pH sensors in plants. *Frontiers in Plant Science* **4**: 523.

Martinière A, Gibrat R, Sentenac H, Dumont X, Gaillard I, Paris N. 2018. Uncovering pH at both sides of the root plasma membrane interface using noninvasive imaging. *Proceedings of the National Academy of Sciences, USA* **115**: 6488–6493.

Mathieu Y, Guern J, Pean M, Pasquier C, Beloeil J-C, Lallemand J-Y. 1986. Cytoplasmic pH regulation in *Acer pseudoplatanus* cells: II. Possible mechanisms involved in pH regulation during acid-load. *Plant Physiology* **82**: 846–852.

McClure PR, Kochian LV, Spanswick RM, Shaff JE. 1990. Evidence for cotransport of nitrate and protons in maize roots: I. Effects of nitrate on the membrane potential. *Plant Physiology* **93**: 281–289.

Millenaar FF, Lambers H. 2003. The alternative oxidase: *in vivo* regulation and function. *Plant Biology* **5**: 2–15.

Moseyko N, Feldman LJ. 2001. Expression of pH-sensitive green fluorescent protein in *Arabidopsis thaliana*. *Plant, Cell & Environment* **24**: 557–563.

Munns R, Day DA, Fricke W, Watt M, Arsova B, Barkla BJ, Bose J, Byrt CS, Chen ZH, Foster KJ *et al.* 2019. Energy costs of salt tolerance in crop plants. *New Phytologist*. doi: 10.1111/nph.15864.

Newman IA. 2001. Ion transport in roots: measurement of fluxes using ion-selective microelectrodes to characterize transporter function. *Plant, Cell & Environment* **24**: 1–14.

Newman JR, Raven JA. 1993. Carbonic anhydrase in *Ranunculus penicillatus* spp. *pseudofluitans*: activity, location and implications for carbon assimilation. *Plant, Cell & Environment* **16**: 491–500.

Peters WS, Felle H. 1991. Control of apoplast pH in corn coleoptile segments. I: the endogenous regulation of cell wall pH. *Journal of Plant Physiology* **137**: 655–661.

Peuke AD, Glaab J, Kaiser WM, Jeschke WD. 1996. The uptake and flow of C, N and ions between roots and shoots in *Ricinus communis* L. IV. Flow and metabolism of inorganic nitrogen and malate depending on nitrogen nutrition and salt treatment. *Journal of Experimental Botany* **47**: 377–385.

Poorter H, der Werf AV, Atkin OK, Lambers H. 1991. Respiratory energy requirements of roots vary with the potential growth rate of a plant species. *Physiologia Plantarum* **83**: 469–475.

Pu X, Lv X, Tan T, Fu F, Qin G, Lin H. 2015. Roles of mitochondrial energy dissipation systems in plant development and acclimation to stress. *Annals of Botany* **116**: 583–600.

Qiu Q-S, Barkla BJ, Vera-Estrella R, Zhu J-K, Schumaker KS. 2003. Na^+/H^+ exchange activity in the plasma membrane of *Arabidopsis*. *Plant Physiology* **132**: 1041–1052.

Ramesh SA, Tyerman SD, Gilliham M, Xu B. 2017. γ-Aminobutyric acid (GABA) signalling in plants. *Cellular and Molecular Life Sciences* **74**: 1577–1603.

Rao TP, Yano K, Iijima M, Yamauchi A, Tatsumi J. 2002. Regulation of rhizosphere acidification by photosynthetic activity in cowpea (*Vigna unguiculata* L. Walp.) seedlings. *Annals of Botany* **89**: 213–220.

Raven JA. 1985. Regulation of pH and generation of osmolarity in vascular plants: a cost-benefit analysis in relation to efficiency of use of energy, nitrogen and water. *New Phytologist* **101**: 25–77.

Raven JA. 1986. Biochemical disposal of excess H^+ in growing plants? *New Phytologist* **104**: 175–206.

Raven JA, Doblin MA. 2014. Active water transport in unicellular algae: where, why, and how. *Journal of Experimental Botany* **65**: 6279–6292.

Raven JA, Newman JR. 1994. Requirement for carbonic anhydrase activity in processes other than photosynthetic Inorganic carbon assimilation. *Plant, Cell & Environment* **17**: 123–130.

Raven JA, Smith FA. 1976. Nitrogen assimilation and transport in vascular land plants in relation to intracellular pH regulation. *New Phytologist* **76**: 415–431.

Renault H, Roussel V, El Amrani A, Arzel M, Renault D, Bouchereau A, Deleu C. 2010. The *Arabidopsis pop2-1*mutant reveals the involvement of GABA transaminase in salt stress tolerance. *BMC Plant Biology* **10**: 20.

Rodríguez-Navarro A. 2000. Potassium transport in fungi and plants. *Biochimica et Biophysica Acta, Reviews on Biomembranes* **1469**: 1–30.

Sakano K. 1998. Revision of biochemical pH-stat: involvement of alternative pathway metabolisms. *Plant and Cell Physiology* **39**: 467–473.

Sakano K. 2001. Metabolic regulation of pH in plant cells: role of cytoplasmic pH in defense reaction and secondary metabolism. In: Jeon KW, ed. *International review of cytology*. San Diego, CA, USA: Academic Press, 1–44.

Sakano K, Yazaki Y, Mimura T. 1992. Cytoplasmic acidification induced by inorganic phosphate uptake in suspension cultured *Catharanthus roseus* cells: measurement with fluorescent pH indicator and 31P-nuclear magnetic resonance. *Plant Physiology* **99**: 672–680.

Schaaf G, Ludewig U, Erenoglu BE, Mori S, Kitahara T, von Wirén N. 2004. *ZmYS1* functions as a proton-coupled symporter for phytosiderophore- and Nicotianamine-chelated metals. *Journal of Biological Chemistry* **279**: 9091–9096.

Schulte A, Lorenzen I, Böttcher M, Plieth C. 2006. A novel fluorescent pH probe for expression in plants. *Plant Methods* **2**: 7.

Serrano R. 1989. Structure and function of plasma membrane ATPase. *Annual Review of Plant Physiology and Plant Molecular Biology* **40**: 61–94.

Shabala L, Cuin TA, Newman IA, Shabala S. 2005. Salinity-induced ion flux patterns from the excised roots of *Arabidopsis sos* mutants. *Planta* **222**: 1041–1050.

Shabala S, Chen G, Chen Z-H, Pottosin I. 2019. The energy cost of the tonoplast futile sodium leak. *New Phytologist*. doi: 10.1111/nph.15758.

Shabala S, Newman I. 2000. Salinity effects on the activity of plasma membrane H^+ and Ca^{2+} transporters in bean leaf mesophyll: masking role of the cell wall. *Annals of Botany* **85**: 681–686.

Shabala S, Newman I, Whittington J, Juswono U. 1998. Protoplast ion fluxes: their measurement and variation with time, position and osmoticum. *Planta* **204**: 146–152.

Shabala SN, Newman IA. 1997. Proton and calcium flux oscillations in the elongation region correlate with root nutation. *Physiologia Plantarum* **100**: 917–926.

Shelp BJ, Bown AW, McLean MD. 1999. Metabolism and functions of gamma-aminobutyric acid. *Trends in Plant Science* **4**: 446–452.

Sklenar J, Fox GG, Loughman BC, Pannifer ADB, Ratcliffe RG. 1994. Effects of vanadate on the ATP content, ATPase activity and phosphate absorption capacity of maize roots. *Plant and Soil* **167**: 57–62.

Smith FA, Raven JA. 1979. Intracellular pH and its regulation. *Annual Review of Plant Physiology* **30**: 289–311.

Snedden WA, Chung I, Pauls RH, Bown AW. 1992. Proton/l-glutamate symport and the regulation of intracellular pH in isolated mesophyll cells. *Plant Physiology* **99**: 665–671.

Sun J, Dai S, Wang R, Chen S, Li N, Zhou X, Lu C, Shen X, Zheng X, Hu Z *et al.* 2009. Calcium mediates root K^+/Na^+ homeostasis in poplar species differing in salt tolerance. *Tree Physiology* **29**: 1175–1186.

Taiz L, Zeiger E. 2010. *Plant physiology, 5th edn.* Sunderland, MA, USA: Sinauer Assn.

Tang X, Yang X, Li H, Zhang H. 2018. Maintenance of K^+/Na^+ balance in the roots of *Nitraria sibirica* Pall. in response to NaCl Stress. *Forests* **9**: 601.

Thibaud J-B, Davidian J-C, Sentenac H, Soler A, Grignon C. 1988. H^+ cotransports in corn roots as related to the surface pH shift induced by active H^+ excretion. *Plant Physiology* **88**: 1469–1473.

Thomine S, Schroeder JI. 2013. *Plant metal transporters with homology to proteins of the NRAMP family*. Austin, TX, USA: Landes Bioscience.

Touraine B, Muller B, Grignon C. 1992. Effect of phloem-translocated malate on NO_3^- uptake by roots of intact soybean plants. *Plant Physiology* **99**: 1118–1123.

Ueda A, Shi W, Sanmiya K, Shono M, Takabe T. 2001. Functional analysis of salt-inducible proline transporter of barley roots. *Plant and Cell Physiology* **42**: 1282–1289.

Ullrich-Eberius CI, Novacky A, Fischer E, Lüttge U. 1981. Relationship between energy-dependent phosphate uptake and the electrical membrane potential in *Lemna gibba* G1. *Plant Physiology* **67**: 797–801.

Volkov V. 2015. Salinity tolerance in plants. Quantitative approach to ion transport starting from halophytes and stepping to genetic and protein engineering for manipulating ion fluxes. *Frontiers. Plant Science* **6**: 873.

Wegner LH. 2014. Root pressure and beyond: energetically uphill water transport into xylem vessels? *Journal of Experimental Botany* **65**: 381–393.

Wegner LH. 2015. A thermodynamic analysis of the feasibility of water secretion into xylem vessels against a water potential gradient. *Functional Plant Biology* **42**: 828–835.

Wegner LH. 2017. Cotransport of water and solutes in plant membranes: the molecular basis, and physiological functions. *AIMS Biophysics* **4**: 192–209.

Wegner LH, De Boer AH, Raschke K. 1994. Properties of the K^+ inward rectifier in the plasma membrane of xylem parenchyma cells from barley roots: effects of TEA^+, Ca^{2+}, Ba^{2+} and La^{3+}. *The Journal of Membrane Biology* **142**: 363–379.

Weisenseel MH, Dorn A, Jaffe LF. 1979. Natural H^+ currents traverse growing roots and root hairs of barley (*Hordeum vulgare* L.). *Plant Physiology* **64**: 512–518.

Wu H, Zhang X, Giraldo JP, Shabala S. 2018. It is not all about sodium: revealing tissue specificity and signalling roles of potassium in plant responses to salt stress. *Plant and Soil* **431**: 1–17.

Yang Y, Hammes UZ, Taylor CG, Schachtman DP, Nielsen E. 2006. High-affinity auxin transport by the AUX1 influx carrier protein. *Current Biology* **16**: 1123–1127.

Yu Q, Tang C, Chen Z, Ku J. 1999. Extraction of apoplastic sap from plant roots by centrifugation. *New Phytologist* **143**: 299–304.

Key words: active pH buffering, carboanhydrase, GABA shunt, malic enzyme, microelectrode ion flux estimation (MIFE), net H^+ influx, proton motive force, P-type H^+ ATPase (proton pump).

Received, 7 April 2019; accepted, 1 August 2019.